Complete Determination of Polarization for a High-Energy Deuteron Beam*

JANICE BUTTON
Lawrence Radiation Laboratory, Berkeley, California

AND

RONALD MERMOD
CERN, Geneva, Switzerland

(Received December 2, 1959)

Double-scattering measurements have been made which yielded all parameters necessary to describe completely the interaction of the deuteron with complex nuclei. Deuterons of 410 and 420 Mev were scattered from beryllium and carbon, respectively. Tensor components of polarization, which should appear in the scattering of spin-1 particles and which were unobservable at low energies, were determined to be appreciably different from zero. The usual vector spin polarization normal to the plane of scattering was found to reach a maximum of about 70%. The impulse approximation was employed to obtain estimates of deuteron cross section and polarization on the basis of nucleon scattering data.

I. INTRODUCTION

MANY studies have been made of the spin-orbit potential in nucleon interactions.[1] Experimental work on the scattering of deuterons has been rather limited; Baldwin et al.[2] measured cross sections and polarizations for deuteron scattering from various elements at 94, 125, and 157 Mev, but did not observe any of the "tensor components" of polarization expected for a spin-1 particle. Stapp investigated extensively the application of the impulse approximation and from nucleon data obtained good predictions at 157 Mev of deuteron cross section, but not of polarization.[3,4]

Scattering measurements at a deuteron energy above 400 Mev, available from the modified 184-in. cyclotron, seemed desirable to determine whether the tensor components of polarization might be observable; further, a method of using magnetic bending between scatterings to separate the two components of polarization appearing in the $\cos\phi$ asymmetry was suggested.

Results of such experiments with high-energy deuterons are reported here. They concern the scattering by beryllium and carbon of two polarized beams having different tensor components resulting from different amounts of bending in a magnetic field. An analysis is carried out on the basis of the impulse approximation and comparison made with Baldwin's results.

II. THEORY

The theory of polarization of the deuteron was first developed by Lakin[5] and subsequently treated with a different formalism by Stapp.[3] With a spin-zero target nucleus, four independent matrices are necessary to specify the scattering matrix of nucleons having a two-dimensional spin space; similarly, there must be nine linearly independent matrices to describe the scattering of deuterons, which have a three-dimensional spin space. The application of parity and time-reversal restrictions reduces this number to five. For the nucleons, the unit matrix and the three Pauli spin operators suffice, but for the deuteron there must be included in the scattering matrix not only terms linear in the spin operators, but second-rank tensor terms as well.

A convenient set of operators given by Lakin includes the unit matrix, two linear combinations of spin operators, and three second-rank tensor products of spin operators, as well as the Hermitian adjoint of three of these. The advantages of this particular representation are that these irreducible operators transform in spin space just as the spherical harmonics transform in coordinate space, and further that the second-scattered intensity may be simply expressed in terms of their expectation values.

As functions of the usual spin-1 operators, those of Lakin are:

$$\begin{aligned} T_{00}&=1,\\ T_{11}&=-(\sqrt{3}/2)(S_x+iS_y),\\ T_{10}&=(\tfrac{3}{2})^{\frac{1}{2}}S_z,\\ T_{22}&=(\sqrt{3}/2)(S_x+iS_y)^2,\\ T_{21}&=-(\sqrt{3}/2)[(S_x+iS_y)S_z+S_z(S_x+iS_y)],\\ T_{20}&=(1/\sqrt{2})(3S_z^2-2),\\ T_{J,-M}&=(-)^M T_{JM}{}^\dagger. \end{aligned} \tag{1}$$

The T_{JM} spin operators may be substituted for the R operators in the general expression for the differential cross section in second scattering,[6]

$$I_2=\frac{1}{n_i}\sum_\nu \langle R^\nu\rangle_i \,\mathrm{Tr}M^\dagger M R^{\nu\dagger}, \tag{2}$$

* Work done under the auspices of the U. S. Atomic Energy Commission.

[1] W. B. Riesenfeld and K. M. Watson, Phys. Rev. **102**, 1161 (1956). Robert D. Tripp, University of California Radiation Laboratory Report UCRL-2975, April, 1955 (unpublished). O. Chamberlain, E. Segrè, R. D. Tripp, C. Wiegand, and T. Ypsilantis, Phys. Rev. **102**, 1659 (1956).

[2] J. Baldwin, O. Chamberlain, E. Segrè, R. Tripp, C. Wiegand, and T. Ypsilantis, Phys. Rev. **103**, 1502 (1956).

[3] Henry P. Stapp, University of California Radiation Laboratory Report UCRL-3098, August, 1955 (unpublished).

[4] H. P. Stapp, Phys. Rev. **107**, 607 (1957).

[5] W. Lakin, Phys. Rev. **98**, 139 (1955).

[6] L. Wolfenstein and J. Ashkin, Phys. Rev. **85**, 947 (1952).

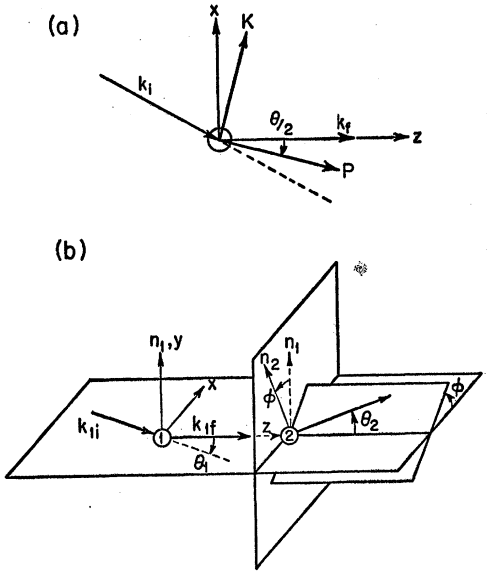

FIG. 1. Geometry of single and double scatterings.

or for the expectation value of a spin operator after single scattering,

$$I_u\langle R^\mu\rangle_f=(1/n_i)\ \mathrm{Tr}MM^\dagger R^\mu. \quad (3)$$

Here n_i is the spin-space dimensionality of the initial system; M is the scattering matrix; and I_u is the differential cross section for scattering of an unpolarized beam.

Lakin chooses a coordinate system in which the y axis is the normal to the scattering plane, $\mathbf{n}=\mathbf{k}_i\times\mathbf{k}_f$, and the z axis is the direction of motion of the once-scattered beam. See Fig. 1. He defines a general form for $M^\dagger M$ and also for $MM^\dagger$ on the basis of invariance arguments and obtains for the second-scattered intensity

$$I_2=I_p(\theta_2,\phi)=I_u(\theta_2)[1+\langle T_{20}\rangle_1\langle T_{20}\rangle_2 +2(\langle iT_{11}\rangle_1\langle iT_{11}\rangle_2-\langle T_{21}\rangle_1\langle T_{21}\rangle_2)\cos\phi +2\langle T_{22}\rangle_1\langle T_{22}\rangle_2\cos2\phi], \quad (4)$$

where ϕ is the azimuthal angle between the normals to the two scattering planes; $\langle T_{JM}\rangle_1$ represents the expectation value of the tensor operator T_{JM} after scattering of an unpolarized beam at an angle θ_1 by Target 1; and $\langle T_{JM}\rangle_2$ is the same quantity for Target 2.

The quantity $\langle iT_{11}\rangle$ is referred to as "vector polarization," while the $\langle T_{2M}\rangle$ are components of "tensor polarization" and are associated with a spin alignment rather than an orientation. The $\langle T_{2M}\rangle$ tensor may be represented by an ellipsoidal surface. See Appendix C and Fig. 2.

By arguments similar to those of Wolfenstein and Ashkin,[6] Stapp defines the most general scattering matrix satisfying invariance requirements as[7]

$$M=a(\theta)+b(\theta)S_in_i +[c(\theta)(n_in_j-\tfrac{1}{3}\delta_{ij})+d(\theta)(P_iP_j-K_iK_j)]S_{ij}. \quad (5)$$

This matrix is useful for estimating polarization components in the impulse approximation and also gives some understanding of the origin of the ϕ dependence of terms in $I_p(\theta_2,\phi)$.

If the coordinate system considered has its y axis along the normal and its x and z axes in the plane of scattering, then $\langle S_y\rangle$ is the only component of spin polarization produced in the scattering of an unpolarized beam; i.e., $\langle S_x\rangle=\langle S_z\rangle=0$. Further, it can be shown that the polarization tensor has one of its principal axes along the y axis, or $\langle S_yS_x\rangle=\langle S_yS_z\rangle=0$.[8]

In a double-scattering experiment, magnetic deflection between the two scatterings causes a transformation among the various $\langle T_{2M}\rangle$ components of polarization. As the z axis is defined by the momentum of the beam incident on the second target, the z and x axes are rotated by the magnetic field; further, the spin axes of the polarization tensor are caused to precess in a plane perpendicular to the field direction. For relativistic particles, the latter effect must include the contribution of Thomas precession.[9] The deflection of the

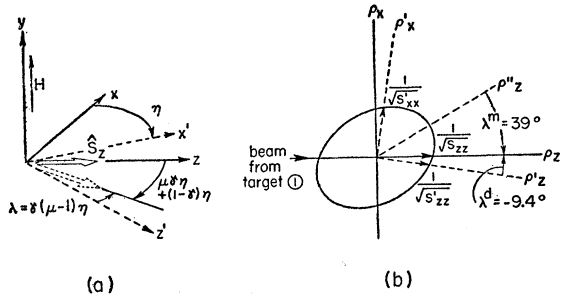

FIG. 2. (a) Rotation of deuteron spin axis under the action of a magnetic field. The initial and final directions of motion of the deuteron are represented by z and z'. (b) Section of polarization ellipsoid in x-z plane of scattering, describing state of polarization after single scattering of an unpolarized beam. The axis ρ_z' is parallel to k_{2i} for the Target d beam; the axis ρ_z'' is parallel to k_{2i} for the Target m beam. (See Fig. 1.) Here S_{zz} is understood to be the expectation value of the square of S_z. [Values of λ refer to beryllium scatterings; they should be multiplied by $\gamma(=1.22)$.]

[7] The **n**, **P**, and **K** are unit vectors forming an orthogonal coordinate system as shown in Fig. 1(a). The S_{ij} are symmetrized spin operators defined as $S_{ij}=\frac{1}{2}(S_iS_j+S_jS_i)-\frac{2}{3}I\delta_{ij}$, with i and j designating x, y, or z of the coordinate system described above. The coefficients $a(\theta)$, etc., may be evaluated in Born approximation from knowledge of the deuteron-nucleus potential and the deuteron wave function.

[8] These operators, which are odd under the parity operation, have zero expectation values after single scattering because terms violating parity conservation and time-reversal invariance are not permitted in the scattering matrix M. The same sort of conclusion cannot be drawn for operators changing sign under time reversal. In the n-P-K coordinate system defined above, the scalar product S_{PK} is odd under time reversal. This means that it cannot appear in the scattering matrix M. However, the S_nS_{KK} and S_nS_{PP} terms of $MM^\dagger$ reduce to S_{PK} and therefore give a nonzero quantity for $\mathrm{Tr}MM^\dagger S_{PK}$. The orientation of the principal axes of the polarization ellipsoid in the plane of scattering would be along the P and K directions, had S_{PK} been required to be zero by time-reversal invariance; instead, the orientation should in general be at some angle to these directions.

[9] Alper Garren, Atomic Energy Commission Report NYO-7102, January, 1955 (unpublished), appendix B.2; James Simmons, Phys. Rev. **104**, 416 (1956).

deuteron in the x-z plane is given by

$$\omega_{\text{cyclotron}}t=\frac{1}{\gamma}\frac{eH}{m_dc}t$$
$$=\frac{1}{\gamma}\frac{eH}{2m_pc}\frac{1}{\gamma}t=\omega_{\text{Larmor}}t\equiv\eta, \quad (6)$$

with t=time and $\gamma=(1-\beta^2)^{-\frac{1}{2}}$. ($\eta$ is positive for deuterons scattered left in a field directed along the positive y axis.) The precession of the spin or magnetic moment is

$$\omega_{\text{precess}}t=[\mu_d\omega_{\text{Larmor}}+(1-\gamma)\omega_{\text{cyclotron}}]t, \quad (7)$$

where μ_d is the magnetic moment of the deuteron in terms of the nuclear magneton. (See Fig. 2.) Thus the angle through which the x-z axes of the polarization tensor are turned relative to the final direction of motion z' is[10]

$$\lambda=(\omega_{\text{precess}}-\omega_{\text{cycl}})t=\gamma(\mu-1)\eta$$
$$=1.22(0.8565-1)\simeq-\tfrac{1}{6}\eta. \quad (8)$$

The effect of the magnetic-field deflection on the second-scattering cross section is determined by using λ to calculate the rotated $\langle T_{2M}\rangle_1'$ quantities which replace the $\langle T_{2M}\rangle_1$ in Eq. (4).

$$\langle T_{20}\rangle'=(1-\tfrac{3}{2}\sin^2\lambda)\langle T_{20}\rangle-(\tfrac{3}{2})^{\frac{1}{2}}\sin2\lambda\langle T_{21}\rangle+(\tfrac{3}{2})^{\frac{1}{2}}\sin^2\lambda\langle T_{22}\rangle,$$
$$\langle T_{21}\rangle'=\tfrac{1}{2}(\tfrac{3}{2})^{\frac{1}{2}}\sin2\lambda\langle T_{20}\rangle+\cos2\lambda\langle T_{21}\rangle-\tfrac{1}{2}\sin2\lambda\langle T_{22}\rangle, \quad (9)$$
$$\langle T_{22}\rangle'=\tfrac{1}{2}(\tfrac{3}{2})^{\frac{1}{2}}\sin^2\lambda\langle T_{20}\rangle+\tfrac{1}{2}\sin2\lambda\langle T_{21}\rangle+\tfrac{1}{2}(1+\cos^2\lambda)\langle T_{22}\rangle.$$

One method of derivation is given in Appendix B.[11] The equivalent ellipsoid rotation is discussed in Appendix C.

III. EXPERIMENT

A double scattering is necessary to determine the polarization components produced in scattering an unpolarized beam of particles. The cross section for deuteron second scattering may be written

$$I_p(\theta_2,\phi)=I_u(\theta_2)(1+d+e\cos\phi+f\cos2\phi), \quad (10)$$

where the parameters d, e, and f contain products of the polarization components which would be produced by scatterings of unpolarized beams at the first and at the second targets. [See Eq. (4).]

The usual double scattering is not sufficient, however, to separate the $\langle iT_{11}\rangle$ and $\langle T_{21}\rangle$ parts of the parameter e. To do this, it is necessary to perform second scatterings of two different polarized beams, one of which has been appreciably changed by the action of a large magnetic field between first and second scatterings.

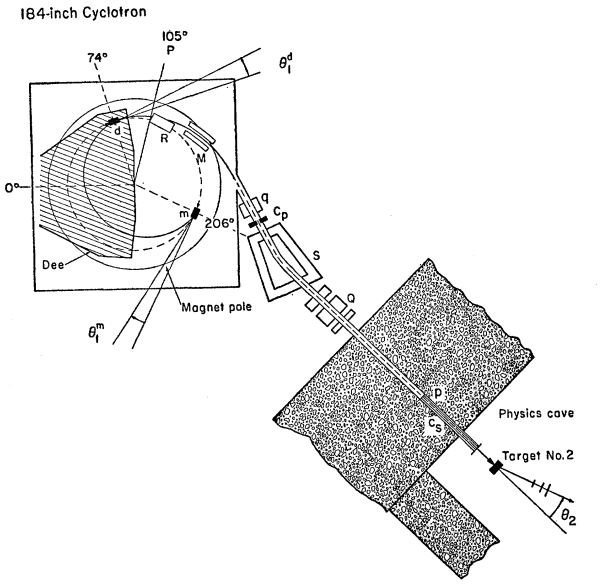

FIG. 3. View of cyclotron and paths of polarized beams. Designated in the figure are: d, target used for left scattering; m, target used for right scattering; R, regenerator; M, magnetic channel; S, steering magnet; Q, 4-inch quadrupole; c_p, premagnet collimator; and c_s, snout collimator.

An essential part of the work reported here was the use of the magnetic field of the cyclotron to produce differing polarization of two scattered beams. The first target scattered left from a position close to the exit channel; the second was located some 230 deg back of the first and scattered to the right a beam which passed through the position used for the first target. The magnitude of scattering angle and the momentum selected were the same in both cases. See Figs. 3 and 4.

Measurements with beryllium targets were made at an energy of 410 Mev with an internal scattering angle of 11 deg. A later set with carbon targets was at an energy of about 420 Mev and a first-scattering angle of 10 deg. Second-scattering angles ranged from 6 to 18 deg and included the diffraction minimum. Unlike the results of Baldwin et al.[2] at lower energies, the cross-section parameters d, e, and f were all found to differ considerably from zero; the angular dependence of each was similar for beryllium and carbon.

An attempt was made to scatter a beam from a target in the steering magnet in order to eliminate the effects of the cyclotron magnetic field and perhaps some systematic errors. However, this was found impractical because of an appreciable high-energy tail and also considerable low-energy contamination.

An estimate was made from Baldwin's data that the scattering angle for maximum polarization at 400 Mev would be 10 or 11 deg. To avoid regenerator action but

[10] It was suggested by Dr. V. Telegdi that there might be a further contribution to the rotation of spin axes by the action of an electric field gradient in the deuteron rest frame on the quadrupole moment of the deuteron, this gradient resulting from the strongly varying magnetic field gradient observed in the laboratory frame. (See Fig. 3.) The average frequency of rotation is $Q\langle dE/dx\rangle_{\text{av}}/\hbar$ and is found to be smaller by a factor of more than 10^{14} than the frequency $\omega_{\text{Larmor}}=\mu H/\hbar$.

[11] Note that the sign of each $\sin2\lambda$ term is opposite to that given by Baldwin.[2,12]

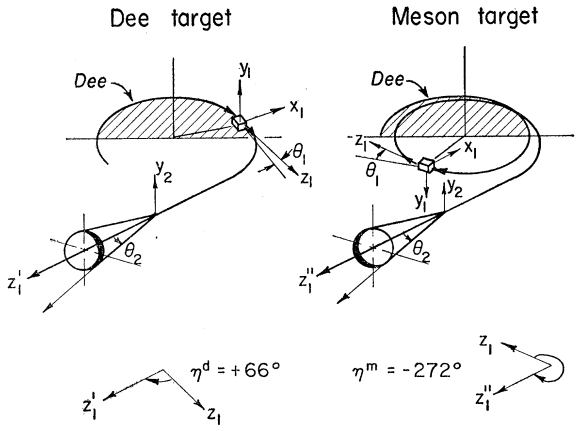

FIG. 4. Pictorial representation of Target d and Target m double scatterings. Cones represent scattering of particles into angle θ_2 at Target 2 with the darker portions indicating greater intensity of particles. The value of the deflection angle η is given in the $x_1y_1z_1$ system in each figure. (These values refer to beryllium scatterings, those for carbon being slightly lower in magnitude.)

obtain maximum energy, 81 inches was chosen as the greatest permissible radius. These choices of scattering angle and radius then determined the target azimuthal position and the momentum of the scattered beam, which were well defined by the exit channel because of the steep field gradients of the regenerator and magnetic-channel regions. Orbits showed that a beam of $H\rho = 1.70 \times 10^6$ gauss-in. scattered left at 11 deg from a target at 74 deg azimuth and also a beam scattered right at 11 deg from 210 deg azimuth passed into the exit tube and through the beam-defining premagnet collimator. (See Target d and Target m in Fig. 3.)

The uncertainties in scattering angle arising from target-positioning errors, from radial oscillations of the circulating beam, and from the momentum acceptance

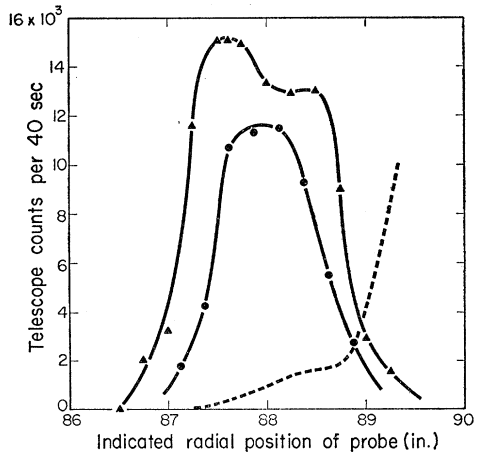

FIG. 5. Variation of beam intensity with radial position of copper probe. The dotted curve represents one-tenth the intensity of the regenerated beam observed with Target d and Target m withdrawn. Circles designate the beam from Target d; triangles, the beam from Target m. The position of the hole in the probe was at a radius $\frac{5}{8}$ in. greater than the indicated reading; the edge clipping the regenerated beam, at a radius 5 in. less than indicated.

of the premagnet collimator gave a total rms uncertainty in angle of 0.50 deg for Target d and 0.60 deg for Target m.

The radial position of a copper collimator ("probe"), put at 105-deg azimuth to stop regenerated beam and pass scattered beam, served as an experimental check on the orbit of the deuterons scattered by Target d. See Fig. 5. The azimuthal position of Target m was optimized after the 105-deg probe was set as earlier required by the beam from Target d.

The premagnet collimator (c_p in Fig. 3) had a 2×3-in. (horizontal-by-vertical) opening. The snout collimator (c_s in Fig. 3) was 1 in. in diameter and 46 in. long. With 1-in. thick internal targets, polarized beam intensities were about 10^5/sec.

A range curve of the beam scattered from the beryllium Target d showed it to have an energy of 410±2.5 Mev. See Fig. 6. The energy of the beam from Target m was 411±4.3 Mev. The degraded regenerated (unpolarized) beam matched the polarized beams well with an energy of 410±2.1 Mev.

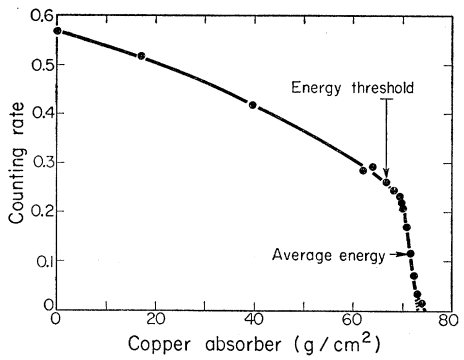

FIG. 6. Range curve of beam scattered by Target d (beryllium). The energy was found equal to 410±2.5 Mev. The energy threshold indicates the amount of absorber (except for recoil correction) used for scattering measurements.

Because of changes in the cyclotron magnetic field caused by a short in the main-field windings, the internal scattering angle in the later carbon measurements could be only approximately estimated as 10 deg. Energies of the polarized beams from Targets d and m were 416 and 422 Mev, respectively, with energy spreads comparable to those for the earlier measurements.

Degrading of the regenerated beam was accomplished by placing several inches of polyethylene absorber at the entrance to the snout collimator. It was not attempted to match polarized and unpolarized beams exactly in energy and energy spreads. Greater values of d and f required less concern over such techniques than in the experiment of Baldwin et al.[2,12]

The scattering table used was similar to that described in a report of earlier polarization work by Chamberlain et al.[1] Rigidity of the apparatus was such

[12] John Baldwin, University of California Radiation Laboratory Report UCRL-3412, May, 1956 (unpublished).

that counter misalignment caused by rotation should not have given more than a 0.02-deg error in θ_2. Unlike the situation in nucleon scattering, the 0.1-deg error in the setting of this polar angle θ_2 could produce errors in the deuteron cross-section parameters, since the ratio of polarized to unpolarized cross sections entered into the determination of each quantity.

The second target was generally $\frac{1}{2}$ in. or $\frac{3}{4}$ in. thick. The counter telescope consisted of three plastic scintillators viewed by 1P21 photomultiplier tubes; the defining counter measured 1×6 in. and was placed 43.5 in. from the target. Sufficient copper absorber was put between Counters 1 and 2 to stop most of the inelastically scattered deuterons, the amount being varied slightly with scattering angle to compensate for changing recoil loss in the target. The rms uncertainty in the

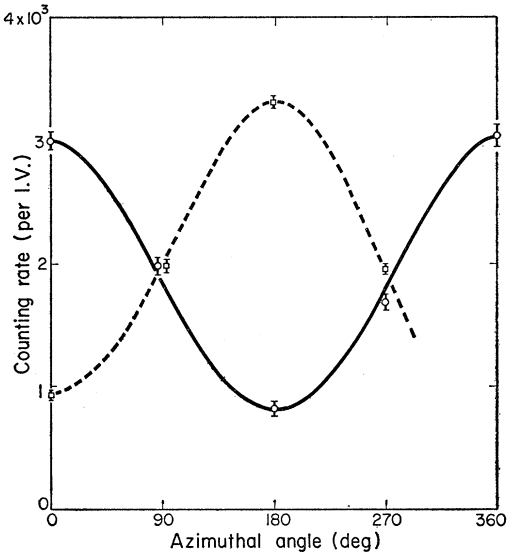

FIG. 7. Polarized cross section vs azimuthal angle for scattering from beryllium at an angle of 8 deg. The solid line represents Target d scattering; the dotted line, Target m scattering.

angle θ due to multiple scattering, to finite counter width, and to beam width was 0.75 deg.

Alignment was accomplished by taking x-ray pictures of the beam at the front and back of the table and by comparing counting rates, left, right, up, and down, at small values of θ. The estimated alignment accuracy was 0.06 deg with the x-ray pictures and 0.03 deg with the counters.

In scattering measurements, an argon-filled ion chamber was used as monitor, with a "multiplication factor" of 1240 for 410-Mev deuterons.[13] The counting procedure was first to check the alignment by measuring the unpolarized beam cross section I_u at an angle of 11 deg with $\phi=0$ deg (left), 90 deg (up), 180 deg (right), and 270 deg (down) and then to measure other $I_u(\theta_2)$ at $\phi=0$. Polarized beam measurements were made at

[13] O. Chamberlain, E. Segrè, and C. Wiegand, Phys. Rev. **83**, 928 (1951).

TABLE I. Asymmetries in polarized-beam scattering. Here $e/(1+d+f)$ is the usual "left-right" asymmetry $(I_0-I_{180})/(I_0+I_{180})$; $f/(1+d)$ is "horizontal-vertical" asymmetry. Errors are statistical.

	Dee target		Meson target	
θ_2	$e/(1+d+f)$	$f/(1+d)$	$e/(1+d+f)$	$f/(1+d)$
Beryllium				
6°	0.411±0.016	−0.003±0.012	0.487±0.013	0.050±0.008
8°	0.555±0.014	0.055±0.009	0.562±0.011	0.041±0.008
10°	0.432±0.024	0.070±0.021	0.488±0.016	0.078±0.012
11°	0.322±0.016	0.069±0.012	0.448±0.010	0.065±0.010
12°	0.294±0.034	0.073±0.025	0.312±0.022	0.085±0.017
14°	0.213±0.032	0.105±0.024	0.185±0.026	0.087±0.020
16°	···	···	0.206±0.030	0.101±0.024
Carbon				
6°	0.320±0.013	0.040±0.010	0.444±0.010	0.035±0.009
8°	0.402±0.021	0.096±0.024	···	···
9°	0.329±0.023	0.125±0.019	0.458±0.023	0.054±0.017
11°	0.167±0.030	0.095±0.025	0.258±0.026	0.098±0.021
13°	0.114±0.047	0.022±0.035	0.201±0.033	0.069±0.025
16°	0.170±0.084	0.089±0.075	0.212±0.040	0.065±0.030
18°	···	···	0.182±0.042	0.105±0.035

the four azimuthal settings for every θ_2. Results near $\theta_2=\theta_1$ were determined especially carefully, as the $\langle T_{JM}\rangle(\theta_1)$ values obtained from these were to be used in finding $\langle T_{JM}\rangle(\theta)$ from measurements at other θ_2.

Three counting rates were measured at each (θ,ϕ) setting: "target in" with normal delay, "target in" with 76 mμsec delay added to one counter, and "target out." Accidental coincidences were generally about 5% of the normal-delay measurements, while the background was about 10%.

Results for the polarized and unpolarized beams at the various ϕ angles were used to obtain the desired cross-section parameters[14] at each angle θ_2:

$$d=(\bar{I}_p/I_u)-1=[(I_0+I_{90}+I_{180}+I_{270})/4I_u]-1,$$
$$e=(I_0-I_{180})/2I_u, \qquad (11)$$
$$f=(I_0+I_{180}-I_{90}-I_{270})/4I_u.$$

(The subscripts designate the angle ϕ or refer to polarized or unpolarized measurements.) The plot of polarized-beam cross section vs azimuthal angle at $\theta_2=8$ deg, Fig. 7, shows a large left-right asymmetry. The asymmetry equal to $e/(1+d+f)$ and that equal to $f(1+d)$ are given with statistical errors for beryllium and carbon scatterings in Table I.

Because each of the desired quantities $(1+d)$, e, and f contained the ratio between polarized and unpolarized cross sections, a serious problem arose. Extrapolations to zero telescope absorber were found to differ by about 10% for the polarized and unpolarized beams and to produce a considerable effect in the value of d. It was concluded that the various beams were not equally free from low-energy particles and that the ionization chamber could not be relied upon for absolute measurements needed for the computation of accurate cross sections.

As an alternative to the use of absolute cross sections, the assumption was made that the average polarized and unpolarized cross sections should be equal at 6 deg

[14] Note that the formulas given by Baldwin[2,12] for e and f are incorrect, though valid for the particular results of his experiment.

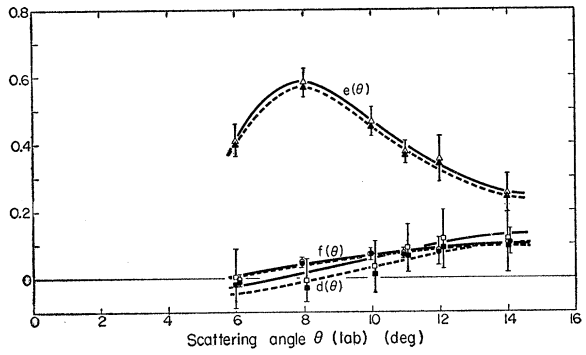

(a)

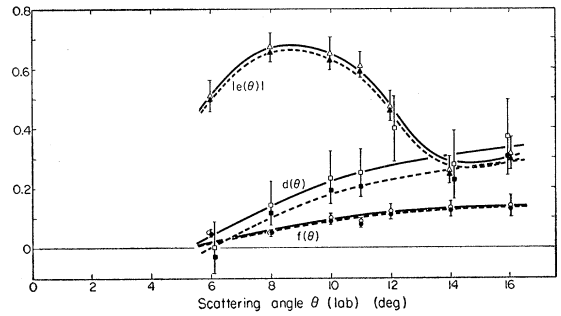

(b)

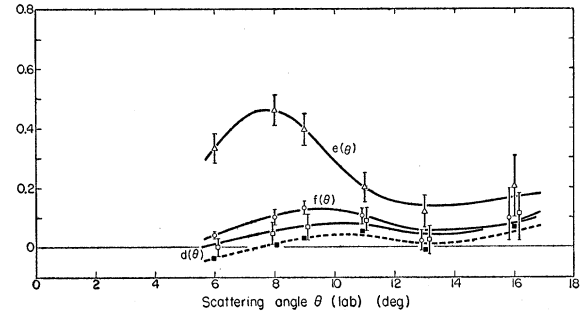

(c)

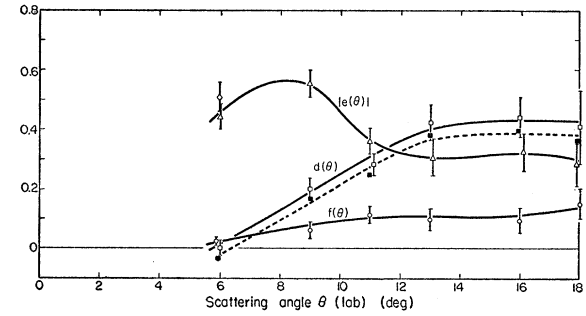

(d)

FIG. 8. Cross-section parameters vs scattering angle obtained with (a) a beryllium Target d and (b) a beryllium Target m at a deuteron energy of 410 Mev; and with (c) a carbon Target d and (d) a carbon Target m at deuteron energies of 416 and 422 Mev, respectively. Solid lines indicate values obtained by normalization; dotted lines, by extrapolation. Errors include systematic as well as statistical effects.

(theory predicting that $\langle T_{20}\rangle$ should go to zero as $\sin^2\theta$); and the unpolarized cross section was normalized to the polarized for all θ. Figure 8 shows the angular dependence of the quantities d, e, and f, which were obtained both by normalization and extrapolation of cross sections. The unpolarized cross sections as functions of scattering angle are given in Fig. 9.

The ratios of counting rate at the energy threshold to that at the average energy of the elastic peak (see Fig. 6) were compared for $\theta=0$ and 10 deg ($\phi=0$). The amount by which they differed indicated that at 10 deg there was an 8% inelastic contamination of the beam above the energy threshold.

Errors in d, e, and f derived chiefly from three sources: statistics of counting, comparison of polarized and unpolarized beams, and misalignment of the scattering apparatus. These are given with values of d, e, and f in Tables II and III. Also, the uncertainty in internal scattering angles gave about 8% error in the quantity $\langle iT_{11}\rangle$.

That accidentals were correctly subtracted was verified by obtaining the same cross-section values at several beam levels. Measurements at ϕ angles of 45, 135, 225, and 315 deg were consistent with those at the usual angles.

IV. ANALYSIS

Measurements of cross sections for each of the two polarized beams gave values of

$$\begin{aligned} d&=\langle T_{20}\rangle_1'\langle T_{20}\rangle_2,\\ e&=2(\langle iT_{11}\rangle_1\langle iT_{11}\rangle_2-\langle T_{21}\rangle_1'\langle T_{21}\rangle_2),\\ f&=2\langle T_{22}\rangle_1'\langle T_{22}\rangle_2, \end{aligned} \tag{12}$$

where primes indicate transformation of the original tensor polarization components by action of the cyclotron field. The asymmetry parameter e in second scattering differed in sign for the beams from Target d and Target m (see Fig. 4). Further, the $\langle iT_{11}\rangle$ and $\langle T_{21}\rangle$ are odd functions of scattering angle θ; and thus the Target m asymmetry was given by

$$e^m/2=-\langle iT_{11}\rangle_1\langle iT_{11}\rangle_2+\langle T_{21}\rangle_1'\langle T_{21}\rangle_2, \tag{13}$$

with all expectation values defined for left scattering and $\langle T_{21}\rangle_1'$ calculated for positive λ.

To eliminate $\langle iT_{11}\rangle$ products from the e parameters obtained by experiment, the expression for the quantity e^d was added to that for e^m to give

$$(e^m+e^d)/2=(\langle T_{21}\rangle_1'^m-\langle T_{21}\rangle_1'^d)\langle T_{21}\rangle_2. \tag{14}$$

This expression with the four remaining experimental quantities gave a system of quadratic equations for the determining of the $\langle T_{2M}\rangle$ at $\theta_2=\theta_1$.

To illustrate the method of calculation, the scatterings from carbon targets with $\theta_1=10$ deg and with $\theta_2=10$ and 9 deg will be considered. Cross-section

values obtained by using Target d with $\theta_1=\theta_2=10$ deg were:

$$\begin{aligned} I_0 &= 333 \text{ counts per unit beam,}^{15} \\ I_{90} &= 232, \\ I_{180} &= 209, \\ I_{270} &= 205; \end{aligned} \tag{15}$$

and the unpolarized cross section was

$$I_u = 212 \text{ counts per unit beam.}$$

As the average polarized cross section and unpolarized cross sections at 6 deg gave a ratio of

$$\bar{I}_p/I_u = 2825/2675 = 1.057, \tag{16}$$

the value of $I_u(10°)$ was normalized to 225. The cross-section parameters then obtained for $\theta_2=10$ deg were

$$\begin{aligned} d^d &= 245/225-1=0.088, \\ e^d &= (333-209)/2\times225=0.276, \\ f^d &= (333+209-232-205)/4\times225=0.117. \end{aligned} \tag{17}$$

By a similar procedure, parameters for scattering of the polarized beam from the meson target were found to be

$$\begin{aligned} d^m &= 0.250, \\ e^m &= -0.464, \\ f^m &= 0.092. \end{aligned} \tag{18}$$

Knowledge of the effective angle of spin rotation for beams from Targets d and m, -11.9 and $+48$ deg, respectively, then gave the rotated tensor components of Eq. (9) and the following quadratic expressions for the measured parameters:

$$\begin{aligned} d^d &= (0.936\langle T_{20}\rangle+0.494\langle T_{21}\rangle+0.052\langle T_{22}\rangle)_1\langle T_{20}\rangle_2, \\ d^m &= (0.158\langle T_{20}\rangle-1.22\langle T_{21}\rangle+0.687\langle T_{22}\rangle)_1\langle T_{20}\rangle_2, \\ e^d &= z(0.247\langle T_{20}\rangle-0.915\langle T_{21}\rangle-0.202\langle T_{22}\rangle)_1\langle T_{21}\rangle_2 \\ &\text{etc.} \qquad +2\langle iT_{11}\rangle_1\langle iT_{11}\rangle_2, \end{aligned} \tag{19}$$

The $\langle iT_{11}\rangle$ were eliminated by the sum:

$$\begin{aligned} e^m+e^d = -0.188 = z(&0.855\langle T_{20}\rangle-1.04\langle T_{21}\rangle \\ &-0.698\langle T_{22}\rangle)_1\langle T_{21}\rangle_2. \end{aligned} \tag{20}$$

The values of the unknown $\langle T_{2M}\rangle$ best fitting the above equations and the remaining two f equations were

$$\begin{aligned} \langle T_{20}\rangle(10°) &= \mp0.405, \\ \langle T_{21}\rangle(10°) &= \pm0.255, \\ \langle T_{22}\rangle(10°) &= \mp0.235. \end{aligned} \tag{21}$$

The rotated $\langle T_{2M}\rangle'(10°)$ given by the expressions in parentheses of Eq. (19) were then calculated and the appropriate d, e, or f value used to determine the $\langle T_{2M}\rangle$

[15] Unit beam is here defined as approximately 5.2×10^7 particles, the number necessary to give a certain quantity of integrated charge collected from the ion chamber; the time required for measurement of I_0 was about 12 minutes.

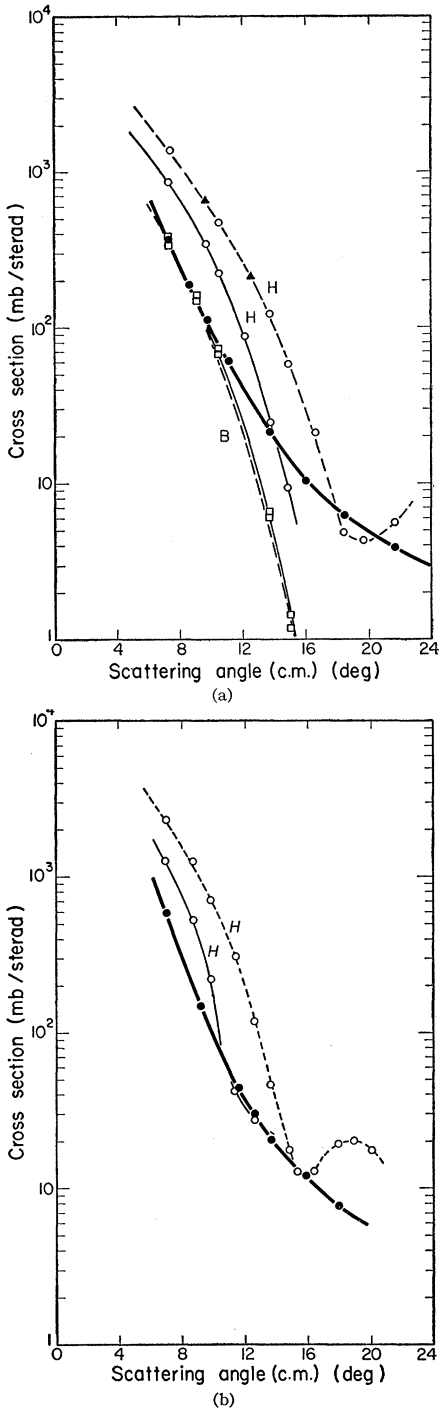

FIG. 9. Cross section for scattering of unpolarized deuterons (a) by beryllium at 410 Mev and (b) by carbon at 425 Mev. Experimental results are designated by solid circles (the size of which is greater than the statistical errors.) Open circles represent calculations done in the impulse approximation with Hafner proton amplitudes, the solid curve including the effect of simultaneous scattering. In (a), the squares represent impulse-approximation results with Bjorklund amplitudes, the solid curve being associated with the proton, and the dotted curve the neutron, amplitudes; both take into account simultaneous scattering. Triangles show the negligible effect of including the deuteron D state in the Hafner calculations.

TABLE II. Cross-section parameters with total errors for scattering from beryllium at 410 Mev.

θ_2	Error in d^d Statistics	Normal-ization	Misalign-ment	$d+\Delta d_{\rm rms}$	Error in e^d Statistics	Normal-ization	Misalign-ment	$e+\Delta e_{\rm rms}$	Error in f^d Statistics	Normal-ization	Misalign-ment	$f+\Delta f_{\rm rms}$
Target d scattering												
6°	0.0629	0.0615	0.0016	0.00 ±0.088	0.0305	0.0253	0.0252	0.411±0.047	0.0127	0.0002	0.0016	−0.003±0.013
8°	0.0204	0.0611	0.0070	−0.006±0.065	0.0146	0.0359	0.0186	0.583±0.043	0.0099	0.0031	0.0070	0.050±0.013
10°	0.0437	0.0636	0.0048	0.034±0.077	0.0279	0.0287	0.0163	0.467±0.043	0.0156	0.0044	0.0048	0.072±0.017
11°	0.0208	0.0670	0.0029	0.090±0.070	0.0194	0.0231	0.0130	0.376±0.033	0.0131	0.0046	0.0029	0.075±0.014
12°	0.0527	0.0687	0.0029	0.117±0.087	0.0636	0.0217	0.0132	0.354±0.068	0.0411	0.0050	0.0029	0.081±0.041
14°	0.0731	0.0687	0.0013	0.117±0.100	0.0543	0.0156	0.0083	0.254±0.057	0.0371	0.0067	0.0013	0.109±0.038
Target m scattering												
	Error in d^m				Error in e^m				Error in f^m			
6°	0.0620	0.0615	0.0027	0.00 ±0.087	0.0336	0.0314	0.0267	−0.510±0.053	0.0083	0.0030	0.0027	0.050±0.009
8°	0.0152	0.0707	0.0068	0.149±0.073	0.0149	0.0413	0.0214	−0.671±0.049	0.0092	0.0029	0.0068	0.047±0.012
10°	0.0470	0.0759	0.0055	0.234±0.089	0.0326	0.0399	0.0200	−0.650±0.055	0.0151	0.0059	0.0055	0.096±0.017
11°	0.0208	0.0769	0.0047	0.250±0.080	0.0177	0.0374	0.0174	−0.609±0.045	0.0119	0.0051	0.0047	0.083±0.014
12°	0.0660	0.0860	0.0043	0.398±0.109	0.0390	0.0291	0.0153	−0.473±0.051	0.0240	0.0073	0.0043	0.119±0.025
14°	0.0826	0.0785	0.0020	0.277±0.114	0.0406	0.0159	0.0109	−0.259±0.045	0.0263	0.0079	0.0020	0.128±0.027
16°	0.0959	0.0841	0.0011	0.367±0.128	0.0492	0.0192	0.0078	−0.312±0.053	0.0341	0.0085	0.0011	0.137±0.035

for other θ_2 angles. Thus at 9 deg, with $d^d=0.068$,

$$\langle T_{20}\rangle(9°)=0.068/\mp 0.201=\mp 0.338. \quad (22)$$

This value was averaged with that from $d^m=0.200$,

$$\langle T_{20}\rangle(9°)=0.200/\mp 0.617\mp\mp 0.324, \quad (23)$$

for the final result.

The d^d and d^m quantities were subject to considerable error; however, IBM calculations showed that the more accurate measurements of e and f were dominant in the analysis and served to determine $\langle T_{20}\rangle(\theta_1)$ to 3% accuracy even if the d measurements were ignored.

As the system of equations for the $\langle T_{2M}\rangle(\theta_1)$ was overdetermined, a least-squares analysis, similar to the Fermi pion-nucleon phase-shift calculation,[16] was used. This required the determination of that combination of $\langle T_{2M}\rangle$ values for which

$$M=\sum_i\left(\frac{x_{\rm exp}{}^i-x_{\rm calc}{}^i}{\Delta x_{\rm exp}{}^i}\right)^2 \quad (24)$$

was a minimum. Here x^i represents the experimental or calculated cross-section parameter and Δx^i the associated error.

Results of the search program are given in Table IV. Four possible sets of $\langle T_{JM}\rangle(\theta_1)$ values were found, as the quadratic nature of the equations left absolute signs in doubt and some cross-terms were small so that certain relative signs were not definitely determined.

The M value associated with each set of solutions and also the probability for finding M larger than this value are given in Table IV. For a good fit, M should be about 2.[17]

The search program was carried out only in those octants of $\langle T_{2M}\rangle$ space indicated by hand calculation as containing solutions. To verify that the four sets of solutions of Cases A and B represented all possible ones, the $f^d/2$ equation, which had a negligible coefficient for the $\langle T_{20}\rangle\langle T_{22}\rangle$ term, was used to plot curves of $\langle T_{22}\rangle$ vs $\langle T_{21}\rangle$ on which any solution had to lie for an arbitrary

TABLE III. Cross-section parameters with total errors for scattering from carbon at 420 Mev.

θ_2	Error in d^d Statistics	Normal-ization	Misalign-ment	$d+\Delta d_{\rm rms}$	Error in e^d Statistics	Normal-ization	Misalign-ment	$e+\Delta e_{\rm rms}$	Error in f^d Statistics	Normal-ization	Misalign-ment	$f+\Delta f_{\rm rms}$
Target d scattering												
6°	0.0214	0.0214	0.0054	0.00 ±0.031	0.0162	0.0071	0.0452	0.333±0.049	0.0098	0.0009	0.0054	0.040±0.011
8°	0.0290	0.0224	0.0088	0.046±0.038	0.0297	0.0099	0.0406	0.461±0.051	0.0241	0.0022	0.0088	0.101±0.026
9°	0.0352	0.0229	0.0098	0.068±0.043	0.0342	0.0085	0.0409	0.396±0.054	0.0210	0.0028	0.0098	0.133±0.023
11°	0.0321	0.0234	0.0050	0.094±0.040	0.0367	0.0043	0.0317	0.201±0.049	0.0266	0.0022	0.0050	0.104±0.027
13°	0.0441	0.0219	0.0019	0.023±0.049	0.0495	0.0026	0.0196	0.119±0.053	0.0352	0.0005	0.0019	0.023±0.035
16°	0.0858	0.0237	0.0002	0.109±0.089	0.1016	0.0044	0.0104	0.205±0.102	0.0797	0.0021	0.0002	0.099±0.080
Target m scattering												
	Error in d^m				Error in e^m				Error in f^m			
6°	0.0165	0.0165	0.0078	0.00 ±0.025	0.0151	0.0071	0.0370	−0.442±0.041	0.0094	0.0007	0.0077	0.024±0.012
9°	0.0309	0.0200	0.0083	0.200±0.038	0.0366	0.0091	0.0252	−0.555±0.045	0.0273	0.0010	0.0080	0.061±0.028
11°	0.0285	0.0215	0.0035	0.284±0.036	0.0378	0.0060	0.0182	−0.363±0.042	0.0287	0.0019	0.0035	0.113±0.029
13°	0.0519	0.0308	0.0037	0.424±0.060	0.0527	0.0066	0.0274	−0.306±0.060	0.0357	0.0021	0.0037	0.098±0.036
16°	0.0597	0.0311	0.0013	0.440±0.067	0.0646	0.0070	0.0109	−0.326±0.066	0.0430	0.0020	0.0013	0.093±0.043
18°	0.1188	0.0304	0.0008	0.407±0.123	0.0722	0.0061	0.0031	−0.281±0.072	0.0499	0.0032	0.0008	0.149±0.050

[16] E. Fermi, N. Metropolis, and E. F. Alei, Phys. Rev. **95**, 1581 (1954).

[17] Peter Cziffra and Michael Moravcsik, University of California Radiation Laboratory Report UCRL-8523, October, 1958 (unpublished).

value of $\langle T_{20}\rangle$. Then M was computed for successive points along the curves. The points at which minima were found corresponded very closely to the A and B solutions.

The rms errors in the $\langle T_{2M}\rangle$ were found by computing the diagonal elements of the inverse of the error matrix.[18] As shown in Table IV, the largest of these was about 20%.

By considering the limitations on the possible statistical weights of the pure states of polarization, Lakin[5] was able to impose a restriction on the $\langle T_{JM}\rangle$ components resulting from single scattering such that any possible state must fall within a truncated cone defined in Lakin's coordinate system by the inequality

$$\langle T_{10}\rangle^2+(\sqrt{2}\langle T_{22}\rangle)^2\leq\tfrac{1}{3}(\langle T_{20}\rangle+\sqrt{2})^2. \quad (25)$$

Without including error estimates, the inequality is satisfied only for the Case B solution with negative $\langle T_{20}\rangle$.

TABLE IV. Best-fit $\langle T_{JM}\rangle$ values and associated M values for $\theta_1=\theta_2$, determined with cross-section parameters calculated from normalized measurements. (Solutions with the same magnitudes but opposite signs for the $\langle T_{2M}\rangle$ components are also possible.)

	Beryllium ($\theta=11°$)		Carbon ($\theta=10°$)	
	Case A	Case B	Case A	Case B
With systematic and statistical errors in d, e, and f				
$\langle T_{20}\rangle$	-0.305 ± 0.070	-0.446 ± 0.050	-0.420 ± 0.090	-0.405 ± 0.030
$\langle T_{21}\rangle$	$+0.210\pm0.025$	$+0.215\pm0.035$	$+0.230\pm0.030$	$+0.255\pm0.026$
$\langle T_{22}\rangle$	$+0.230\pm0.012$	-0.185 ± 0.015	$+0.260\pm0.025$	-0.235 ± 0.014
$\langle iT_{11}\rangle$	$\pm0.494\pm0.012$	$\pm0.502\pm0.010$	$\pm0.425\pm0.024$	$\pm0.465\pm0.020$
M	7.61	3.43	31.3	1.80
$Q(>M)$	0.02	0.18	~0	0.41
With statistical error in d, e, and f[a]				
$\langle T_{20}\rangle$	-0.402 ± 0.022	-0.438 ± 0.007	-0.450 ± 0.038	-0.405 ± 0.016
$\langle T_{21}\rangle$	$+0.233\pm0.013$	$+0.257\pm0.018$	$+0.226\pm0.026$	$+0.270\pm0.052$
$\langle T_{22}\rangle$	$+0.206\pm0.010$	-0.196 ± 0.009	$+0.244\pm0.021$	-0.240 ± 0.011
$\langle iT_{11}\rangle$	$\pm0.498\pm0.007$	$\pm0.515\pm0.007$	$\pm0.430\pm0.014$	$\pm0.465\pm0.014$
M	38.4	14.3	27.3	2.01
$Q(>M)$	0	0.003	0	0.36

[a] These results differ more from the systematic fits than they should because the relativistic Thomas precession effect was not included in calculating the rotated tensor components.

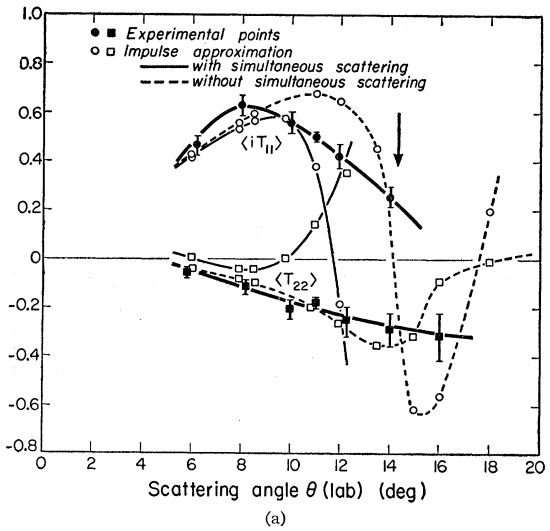

FIG. 10. Polarization components for 410-Mev deuterons scattered by beryllium. Errors on experimental points include statistical and systematic effects. Impulse-approximation calculations were done with Hafner proton amplitudes. The vertical arrow indicates the position of the diffraction minimum. $\langle T_{21}\rangle$ is zero in the usual impulse approximation.

Predictions of tensor-component signs are possible also through use of the impulse approximation. In the first Born approximation, $\langle T_{20}\rangle$ and $\langle T_{22}\rangle$ may be calculated from Eqs. (25) and (28) of the Stapp article. At small angles, they assume forms proportional to θ^2 and can be estimated from nucleon scattering data as

$$\langle T_{20}\rangle=-0.16 \quad \text{and} \quad \langle T_{22}\rangle=-0.22 \quad \text{for } \theta=4 \text{ deg(lab)}. \quad (26)$$

These values again substantiate the choice of the Case B solution.

An examination of the physics of the scattering process helps further to determine the $\langle T_{2M}\rangle$ signs. (Such an argument has been appealed to before in choosing the sign of $\langle iT_{11}\rangle$ positive on the basis of shell-model spin-orbit coupling.)[19] The occupation of the $m_s=0$ state associated with the y axis in the usual coordinate system can be shown to differ from the unpolarized value of $\frac{1}{3}$ by an amount

$$\tfrac{1}{3}-N(0)/N=\tfrac{1}{3}(3\langle S_y^2\rangle-2)=-(1/\sqrt{3})\langle T_{22}\rangle-(1/3\sqrt{2})\langle T_{20}\rangle. \quad (27)$$

For the sign combination of Case A, $N(0)/N$ is very close to $\frac{1}{3}$, while for Case B, it is 0.55 for positive or 0.10 for negative $\langle T_{20}\rangle$. The last of these appears most reasonable. Spin-orbit coupling should cause spin-up particles to be preferentially scattered left, but have no effect on particles with $m_s=0$; however, the absolute fractional occupation of the latter state should in fact be decreased by a left scattering.

[18] H. L. Anderson, W. C. Davidon, M. Glicksmann, and U. E. Kruse, Phys. Rev. **100**, 279 (1955).

[19] Lincoln Wolfenstein, *Annual Review of Nuclear Science* (Annual Reviews, Inc., Palo Alto, 1956), Vol. 6, p. 43.

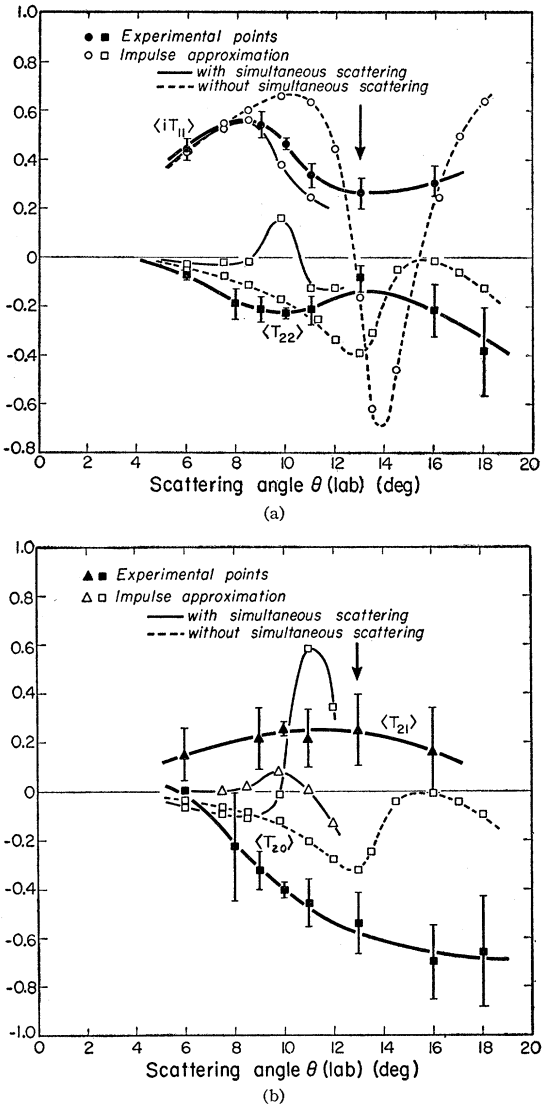

FIG. 11. Polarization components for 420-Mev deuterons scattered by carbon, with impulse-approximation predictions from Hafner proton amplitudes. Total errors are indicated. The arrow designates the diffraction minimum.

The parameter d is observed to increase from near zero to appreciable positive values as θ increases. This behavior might be explained in a simple classical picture by supposing the polarized beam to have a predominant spin alignment transverse to the direction of motion and thus a greater effective geometrical cross section. This argument does not support Case A, but indicates the correctness of the negative $\langle T_{20}\rangle$ Case B solution, for which $\langle S_x^2\rangle=0.63$, $\langle S_y^2\rangle=0.90$, and $\langle S_z^2\rangle=0.48$.

With the negative $\langle T_{20}\rangle$ Case B solutions for $\langle T_{2M}\rangle(\theta_1)$ selected, the $\langle T_{2M}\rangle$ for the other θ were calculated. Averages of Target d and Target m results are plotted with total errors in Figs. 10 and 11.

The internally consistent beryllium results and carbon results, which were obtained under somewhat different conditions, were checked by comparing calculated with measured parameters at several angles θ_2 in a beryllium-carbon double scattering. For only one quantity out of eight examined was the difference between calculated and measured values greater than the experimental error.

V. IMPULSE APPROXIMATION

The matrix describing the scattering of nucleons by complex nuclei may be expressed as

$$M=g(K)+h(K)\boldsymbol{\sigma}\cdot\mathbf{n}, \tag{28}$$

with K the momentum transfer. The quantities $g(K)$ and $h(K)$ take the following forms in Born approximation [provided $V_s(r)/V_c(r)=\text{constant}$]:

$$g(K)=\left(-\frac{m}{2\pi\hbar^2}\right)\int e^{-i\mathbf{K}\cdot\mathbf{r}}V_c(r)d\tilde{r},$$
$$h(K)=i\lambda_c^2k^2\sin\theta\; g(K)\,|V_s(0)|/|V_c(0)|, \tag{29}$$

where $V_c(r)$ is the complex central potential, $V_s(r)$ is the spin-orbit potential, m is the mass of the nucleon, and λ_c is the proton Compton wavelength.

The impulse approximation in deuteron scattering implies the use of a Hamiltonian containing the interaction between the two nucleons, the nucleon-nucleus interaction V_1 for Nucleon 1, and a similar interaction for Nucleon 2. Then, with the assumption that V_1 is equal to V_2, the scattering matrix in Born approximation becomes

$$M_d=\left(-\frac{m_d}{2\pi\hbar^2}\right)\int\int dr_1dr_2\,\chi^*(r_{12})e^{-i\mathbf{k}_f\cdot(1/2)(\mathbf{r}_1+\mathbf{r}_2)}$$
$$\times[V(r_1)+V(r_2)]\,\chi(r_{12})e^{i\mathbf{k}_i\cdot(1/2)(\mathbf{r}_1+\mathbf{r}_2)}$$
$$=f^{\frac{1}{2}}(K)[2g_d(K)+h_d(K,k)\mathbf{S}\cdot\mathbf{n}]. \tag{30}$$

The sticking factor $f(K)$ represents the probability of the deuteron's staying intact during the scattering process.[20]

The $g_d(K)$ and $h_d(K)$ of the deuteron scattering matrix can be expressed in terms of the nucleon scattering amplitudes as

$$g_d(K)=(m_d/m_n)g_n(K),$$
$$h_d(K,k_d)=\left(\frac{k_d}{k_n}\right)^2\frac{\sin\theta_d}{\sin\theta_n}\left(\frac{m_d}{m_n}\right)h_n(K,k_n). \tag{31}$$

There result the formulas,

$$I_u{}^d=f(K)(4|g_d|^2+(2/3)|h_d|^2),$$
$$I_u\langle iT_{11}\rangle=f(K)(2/\sqrt{3})2\,\mathrm{Re}g_d{}^*h_d,$$
$$I_u\langle T_{20}\rangle=-f(K)(1/3\sqrt{2})|h_d|^2, \tag{32}$$
$$I_u\langle T_{21}\rangle=0,$$
$$I_u\langle T_{22}\rangle=-f(K)(1/2\sqrt{3})|h_d|^2.$$

[20] Geoffrey Chew, Phys. Rev. **74**, 809 (1948).

Calculations for deuteron cross sections and polarization components were carried out with the use of nucleon scattering amplitudes obtained from Hafner at Rochester[21] and Bjorklund at Livermore.[22] Both had utilized a Woods-Saxon potential to fit experimental data, but with somewhat differing parameters. The Hafner amplitudes approximated nucleon cross sections much better than those of Bjorklund.

The deuteron cross sections as calculated with Hafner proton amplitudes were larger than experimental measurements by a factor of five or six at small angles. Results with Bjorklund proton and neutron amplitudes dropped too rapidly with angle; but they were very similar, as imaginary amplitudes, unaffected by Coulomb interference, were much larger than real amplitudes. Thus it was assumed that neutron amplitudes were unnecessary in the calculations done with the Hafner data.

Calculations including the deuteron D state were done with the formulas of Stapp.[4] Although the D state should contribute tensor terms to the scattering matrix, results differed inappreciably from those for the S-state wave function alone.

Tensor terms of the scattering matrix arise also from simultaneous scattering of both particles in the deuteron, which gives a contribution to the transition-matrix element proportional to V_1V_2, in addition to the linear combination of V_1 and V_2 of the usual impulse approximation.[4] Inclusion of simultaneous scattering by use of Stapp's formulas in calculations at 410 and 420 Mev reduced beryllium and carbon cross sections to within a factor of 2.5 to 3 of experiment at small angles and brought agreement at moderate angles. However, it gave rather poor results for tensor components of polarization. Predicted $\langle T_{21}\rangle$ values were much smaller than experimental results. (See Figs. 10 and 11.) Near the diffraction minimum, it appeared that the assumptions made by Stapp that the amplitudes for nucleon scattering did not change phase rapidly with angle were not valid.

VI. CONCLUSION

Results for cross section and for polarization components were found very similar for beryllium and carbon, the polarization dependence on angle being somewhat more compressed for the latter. The vector polarization $\langle iT_{11}\rangle$ is plotted in Fig. 12 as a function of the quantity $KA^{\frac{1}{3}}$ for low and high energies of scattering with beryllium and carbon targets. At the higher energies, it was found to reach a maximum at about 8 deg such that $\langle S_y\rangle$ polarization was about 75% for beryllium and 65% for carbon. The $\langle iT_{11}\rangle$ values showed slight evidence of the usual diffraction-minimum behavior observed in nucleon scattering.

[21] E. M. Hafner, Phys. Rev. **111**, 297 (1958) and private communication.

[22] Frank Bjorklund (private communication).

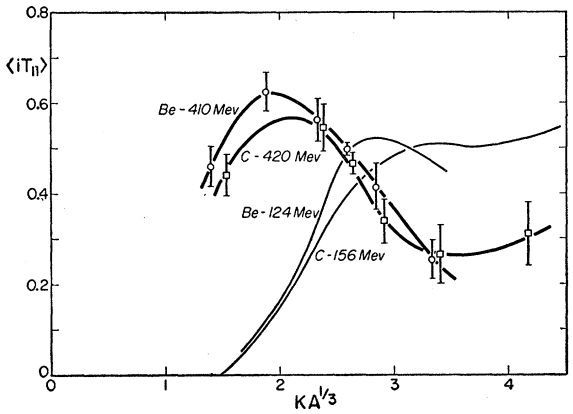

FIG. 12. Vector polarization $\langle iT_{11}\rangle$ vs momentum transfer times $A^{\frac{1}{3}}$.

Besides demonstrating the effects of spin-orbit coupling, complete knowledge of the tensor components in deuteron polarization provides a useful tool for the determination of transition amplitudes in the reaction $p+p\rightarrow\pi^+ +d$ and hence for restrictions on p-p scattering phase shifts.[23] Deuterons of 435 Mev would be produced by this reaction with the 740-Mev protons available at the cyclotron; however, a determination of deuteron polarization using the known analyzabilities of carbon or beryllium at 410 and 420 Mev would be of value only if the formalism assuming S- and P-wave production were revised.[24] Useful information for the analysis of the $p+p\rightarrow\pi^+ +d$ reaction at a proton energy of 415 Mev could be obtained by scattering deuterons at an energy of 420 Mev, degrading, and analyzing at a much lower energy of 235 Mev. As other necessary data are already known,[25] restrictions on p-p scattering phase shifts would then be determined at 415 Mev.

ACKNOWLEDGMENTS

The authors wish to express their appreciation to Professor Owen Chamberlain for excellent advice during the final stages of measurement and analysis of experimental results. Discussions of theoretical problems with Dr. Henry Stapp were of considerable value. Also, the authors thank Professor Emilio Segrè for his interest in the experiment. The assistance of Professor Thomas Ypsilantis, in particular, and also of Dr. Herbert Steiner in carrying out experimental work was much appreciated.

[23] L. Wolfenstein, Phys. Rev. **98**, 766 (1955); F. Mandl and T. Regge, Phys. Rev. **99**, 1478 (1955); F. S. Crawford and M. L. Stevenson, Phys. Rev. **97**, 1305 (1955); R. D. Tripp, Phys. Rev. **107**, 607 (1957).

[24] Yu. K. Akimov, O. V. Savchenko, and L. M. Soroko, Nuclear Phys. **8**, No. 6, 637 (1958); also *1958 Annual International Conference on High-Energy Physics at CERN*, edited by B. Ferretti (CERN, Scientific Information Service, Geneva, 1958), p. 51.

[25] T. H. Fields, J. G. Fox, J. K. Kane, R. A. Stallwood, and R. B. Sutton, Phys. Rev. **96**, 812 (1954).

APPENDIX A. LAKIN INEQUALITY

In a coordinate system with the z axis along the normal to the scattering plane, the pure states of polarization may be described by

$$\psi_1=\chi_0,$$
$$\psi_2=A\chi_{+1}+B\chi_{-1},$$
$$\psi_3=B^*\chi_{+1}-A^*\chi_{-1},$$

with χ_{+1}, χ_0, and χ_{-1} the eigenstates of S_z. If these states have statistical weights of λ_1, λ_2, and λ_3, the density matrix has the form

$$\rho=\begin{bmatrix}\lambda_2A^2+\lambda_3B^2 & 0 & (\lambda_2-\lambda_3)AB^*\\ 0 & \lambda_1 & 0\\ (\lambda_2-\lambda_3)A^*B & 0 & \lambda_2B^2+\lambda_3A^2\end{bmatrix}.$$

Equating terms in this matrix to those in the T_{JM} representation and choosing A and B to be real gives

$$\tfrac{1}{3}[1+(\tfrac{3}{2})^{\frac{1}{2}}\langle T_{10}\rangle+(1/\sqrt{2})\langle T_{20}\rangle]=\lambda_2A^2+\lambda_3B^2,$$
$$\tfrac{1}{3}[1-(\tfrac{3}{2})^{\frac{1}{2}}\langle T_{10}\rangle+(1/\sqrt{2})\langle T_{20}\rangle]=\lambda_3A^2+\lambda_2B^2,$$
$$\langle T_{22}\rangle=\sqrt{3}(\lambda_2-\lambda_3)AB.$$

Obviously, then since $(\lambda_2-\lambda_3)^2\leq(\lambda_2+\lambda_3)^2$, there results

$$\langle T_{10}\rangle^2+(\sqrt{2}\langle T_{22}\rangle)^2\leq\tfrac{1}{3}(\langle T_{20}\rangle+\sqrt{2})^2.$$

APPENDIX B. ROTATION OF THE POLARIZATION TENSOR BY A MAGNETIC FIELD

The simplest method for transforming the $\langle T_{JM}\rangle$ is to express the S_iS_j in terms of the T_{JM} and to carry out an orthogonal transformation representing rotation through the angle λ. [$\lambda=\gamma(\mu-1)\eta$. See Fig. 2.] Just as a spin vector expressed in the x-y-z coordinate system can be transformed for rotation about the y axis by taking

$$\mathbf{S}'=\begin{bmatrix}\cos\lambda & 0 & -\sin\lambda\\ 0 & 1 & 0\\ \sin\lambda & 0 & \cos\lambda\end{bmatrix}\begin{bmatrix}S_x\\ S_y\\ S_z\end{bmatrix}=\mathbf{AS},$$

so the tensor spin products can be transformed with the same matrix $\mathbf{A}$:

$$(\mathbf{SS})'=\mathbf{A}(\mathbf{SS})\mathbf{A}^{-1}.$$

One obtains $(\mathbf{SS})'$ in terms of the original $\mathbf{SS}(T_{JM})$ elements and trigonometric functions of λ. Equating the expressions for each element of $(\mathbf{SS})'$ then gives the formulas included in Baldwin's Appendix[2,12] (though with opposite signs for the sin2λ terms). For example,

$$(\tfrac{1}{3})^{\frac{1}{2}}(-\langle T_{21}\rangle'-2\langle T_{11}\rangle')$$
$$=[-(\tfrac{1}{2})^{\frac{1}{2}}\langle T_{20}\rangle+(\tfrac{1}{3})^{\frac{1}{2}}\langle T_{22}\rangle](\tfrac{1}{2})\sin2\lambda$$
$$+(\tfrac{1}{3})^{\frac{1}{2}}(\langle T_{21}\rangle-2\langle T_{11}\rangle)\sin^2\lambda$$
$$+(\tfrac{1}{3})^{\frac{1}{2}}(-\langle T_{21}\rangle-2\langle T_{11}\rangle)\cos^2\lambda.$$

Thus,

$$\langle T_{21}\rangle'=\langle T_{20}\rangle(\tfrac{1}{2})(\tfrac{3}{2})^{\frac{1}{2}}\sin2\lambda$$
$$+\langle T_{21}\rangle\cos2\lambda-\langle T_{22}\rangle(\tfrac{1}{2})\sin2\lambda.$$

APPENDIX C. POLARIZATION ELLIPSOID

The ellipsoid associated with the polarization tensor $\mathbf{SS}$ is analogous to the moment-of-inertia ellipsoid. It can be represented by a surface whose equation is

$$1=\langle S_x^2\rangle\rho_x^2+\langle S_y^2\rangle\rho_y^2+\langle S_z^2\rangle\rho_z^2$$
$$+(\langle S_xS_y\rangle+\langle S_yS_x\rangle)\rho_x\rho_y+(\langle S_xS_z\rangle+\langle S_zS_x\rangle)\rho_x\rho_z$$
$$+(\langle S_yS_z\rangle+\langle S_zS_y\rangle)\rho_y\rho_z.$$

The effects of rotating the polarization tensor about one of its principal axes can be easily determined by consideration of the rotation of the ellipsoid cross section in the plane perpendicular to this axis. (See Fig. 2.)

As a simple example, the χ_0 eigenfunction of S_x gives expectation values of spin products which are

$$\langle S_x^2\rangle=0,\quad\langle S_z^2\rangle=1,$$
$$\langle S_y^2\rangle=1,\quad\langle S_yS_x\rangle=\langle S_yS_z\rangle=\langle S_xS_z\rangle=0.$$

The reciprocals of $\langle S_x^2\rangle^{\frac{1}{2}}$, $\langle S_y^2\rangle^{\frac{1}{2}}$, and $\langle S_z^2\rangle^{\frac{1}{2}}$ are the ellipsoid axes and in this case form a degenerate ellipsoid, namely, a cylinder of radius 1 extending to plus and minus infinity along the x axis.

If this cylinder is rotated through an angle λ equal to 90 deg, the new ellipsoid should be a cylinder of radius 1 extending to infinity along the z axis. The final value of $\langle S_z^2\rangle'$ after rotation gives

$$\langle T_{20}\rangle'=(1/\sqrt{2})(0-2)=-\sqrt{2}.$$

This agrees exactly with the $\langle T_{20}\rangle'$ found from the first of the rotation equations [see Eq. (9)].

The ellipse corresponding to the Case B solution of the $\langle T_{JM}\rangle(\theta_1)$ equations for carbon gave

$$\langle S_z^2\rangle^{-\frac{1}{2}}=1/\sqrt{S_{zz}''}=1.58$$

for the deflected beam from the meson target. The value of $\langle T_{20}\rangle''$ then was -0.56; the rotation equations gave $\langle T_{20}\rangle''=-0.536$.